Field Test and Evaluation of Model Predictive Control in a Grid-Interactive Thermal Energy Storage Integrated Heat Pump System

Yiyuan QIAO[1], Xiaobing LIU*[1], Jin DONG[1], Liang SHI[2], Lingshi WANG[1], Borui CUI[1], Ming QU[2]

[1]Oak Ridge National Laboratory,
Oak Ridge, TN, USA
qiaoy@ornl.gov
liux2@ornl.gov
dongj@ornl.gov
wangl2@ornl.gov
cuib@ornl.gov

[2]Purdue University, Lyles School of Civil Engineering,
West Lafayette, IN, USA
shi448@purdue.edu
mqu@purdue.edu

* Corresponding Author

ABSTRACT

The grid-interactive heat pump (HP) system is designed to participate in demand response programs, thereby contributing to grid stability. Considering this, thermal energy storage (TES) incorporated with the grid-interactive HP has gained increasing attention due to its capacity for load shifting, energy cost reduction, and improved system flexibility. Efficient management of the TES charge and discharge processes, which is crucial for minimizing total energy costs, requires consideration of various factors such as electricity costs, weather data, and building cooling loads. Therefore, an intelligent control becomes essential for optimizing TES utilization in grid-interactive buildings. In this study, a dynamic model for controlling the TES integrated HP system was developed based on experimental data. A model predictive control (MPC) based on the dynamic programming method was then developed to optimize the performance of the HP-TES system, ensuring both reduced electrical costs and sustained human comfort. This optimal control was evaluated by comparing with a rule-based control (RBC) through field tests in a real building. The results demonstrate that the proposed optimal control strategy exhibits intelligent system operation management by selecting different operation modes under various circumstances. Compared with RBC, it can achieve a 21% decrease in energy consumption in the field test. This paper provides insights for smart control for the grid-interactive HP system.

Keywords: Thermal energy storage, Heat pump, Optimal control, Field test, Grid-interactive system

1. INTRODUCTION

TES (Thermal Energy Storage) integrated systems have gained increasing attention over recent decades due to their ability to efficiently utilize and store energy. These systems can store cooling or heating when energy costs are lower and release it when energy costs are higher (Tarragona *et al.*, 2020; Hirschey *et al.*, 2023). This advantage is

particularly useful for shifting load in response to Time-of-Use (ToU) rates and integrating unstable energy sources, such as renewable energy (Stritih *et al.*, 2018; Shi *et al.*, 2021). Additionally, TES systems can facilitate operations that charge the storage unit when the energy source is readily available and discharge when the regular HVAC system cannot operate normally, such as personal cooling systems (Dhumane *et al.*, 2019; Qiao *et al.*, 2019, 2020).

Existing literature distinguishes Rule-Based Control (RBC) and Model Predictive Control (MPC) as two key approaches in building HVAC systems, enhancing energy efficiency and occupant comfort. RBC, straightforward and easy to implement, may struggle with adapting to changes and optimizing performance (Tarragona *et al.*, 2020; Fu *et al.*, 2023). In contrast, MPC uses a simplified dynamic model to predict and optimize HVAC operations, handling complex system interactions and adjusting to real-time changes effectively (Pangborn, Laird and Alleyne, 2020; Tarragona *et al.*, 2020; Jin *et al.*, 2021; Cui *et al.*, 2022). MPC can be used to optimize the cooling system operation since it can not only optimize the system in the current circumstance but also the future circumstance taking the forecast parameters into consideration. Wang *et al.* (2018) explored MPC in the hybrid free cooling system with TES unit and achieved up to 18% energy saving without sacrificing temperature requirements. Kuboth *et al.* (2019) investigated MPC applied in a complex residential energy system with electrical connectivity to the public grid. The simulation shows that these approaches can achieve 11.6% cost reduction and increase thermal comfort. Despite these advantages, practical field test investigations of MPC in TES-coupled cooling systems are still limited (Tarragona *et al.*, 2021). Contributing to this area, Kim *et al.* (2022) presented MPC demonstration and evaluation of a campus-level district cooling system integrating a chiller plant, TES, and behind-meter photovoltaics, formulated as a mixed-integer linear program for improved control properties.

To address this research gap, this paper applies MPC to a field test on a TES-coupled, grid-interactive heat pump (HP) system, comparing its performance with RBC. The system features four distinct operation modes—HP mode, TES charging, TES discharging, and standby—none of which can operate simultaneously. While both MPC and RBC logically select operation modes based on thermostat settings and electricity costs, this study highlights the performance enhancements achieved through the MPC strategy.

2. METHODOLOGY

This section focuses on the methodology of this study. Section 2.1 describes the TES integrated HP system for the field test. Section 2.2 presents the PCM properties used in the field test and the MPC models. Section 2.3 focuses on the detailed MPC algorithm and the MPC implementation to the TES-HP field test as well as the baseline RBC control logic. Section 2.4 describes the approach to evaluate MPC in the field tests.

2.1 Field test setup

The field test was conducted at a room of Flexible Research Platform (FPR2) in Oak Ridge National Laboratory as shown in Figure 1. The heat pump system used in this study is a dual-source HP system, while in this study only the air source condenser was applied. A direct expansion (DX) coil worked as evaporator and can cool to the room space. Besides the regular HP components, the TES-integrated HP (TES-HP) system in this study has an additional hydronic loop with following specified components:

- A refrigerant-to-water plate heat exchanger, installed as a parallel evaporator of HP system in order to transfer cooling to the hydronic loop and charge a thermal energy storage (TES) unit.
- A TES unit, which is a packed-bed configured PCM-to-water heat exchanger and consisted of 48 PCM-packed vertical tubes and a 50-gallon water tank, as shown in Figure 1.
- A water-to-air fan coil to provide cooling to the room space as discharging the TES unit.
- Other components, such as two pumps and two three-ways to conduct water circulation for the cooling charge and discharge process, respectively.

This TES-HP system can achieve four operation modes as follows:

(1) **HP cooling mode**: HP is ON providing cooling to the room space via DX coil; TES unit is standby.
(2) **TES charge mode**: HP is ON providing cooling to TES unit; TES is charged, and the pump for charging TES is ON.

(3) **TES discharge mode**: HP is OFF; TES is discharged providing cooling to the room space via the water-to-air fan coil; the pump for discharging TES is ON.
(4) **Standby mode**: HP is OFF; Pumps in TES hydronic loops are OFF.

The designed cooling capacity of the HP system is around 2.5 kW, with a fixed compressor speed in the refrigerant loop and fixed pump speeds in the hydronic loop. Therefore, in this study, the primary method for maintaining the thermal state of a building involves the activating or deactivating operation of the cooling system, rather than controlling the flow rate or the instantaneous cooling capacity. The antifreeze solution was used to protect the hydronic loop from freezing, since charging TES required lower evaporator temperature. In the TES unit, the packed-PCM is tube-shaped with the length of 0.9 m and diameter of 0.05 m.

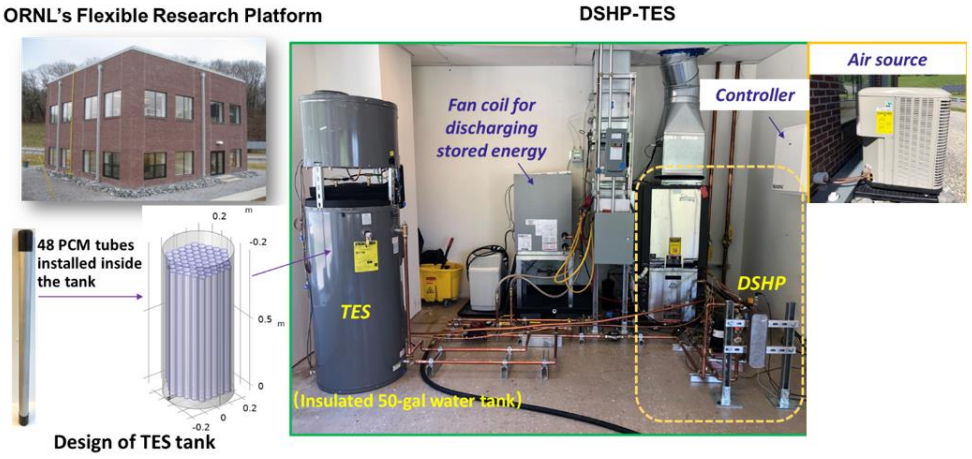

Figure 1: TES-HP Field test system and environment

2.2 PCM properties

The packed PCM in the TES water tank conducts melting process during the discharge mode and get solidified during the cooling charge mode. PCM used in this study is an organic material, i.e., methyl laurate, named Croda Therm 5 from Croda Inc. Its phase-change temperature is around 4 °C, according to the thermal analysis from DSC (Differential Scanning Calorimetry). Other thermal properties are listed in Table 1.

As shown in Figure 2, the specific enthalpy of PCM can be regarded as a function of its temperature. When the temperature is 0 °C, the reference specific enthalpy is set to be 0 kJ/kg. The red line and the blue line described the PCM enthalpy variation during the melting and solidification process, respectively, based on the DSC analysis. To simplify the control-oriented PCM model, the difference of the enthalpy profile between the solidification and the melting process is eliminated, and the enthalpy curve used in this study is shown by the black line, represented by a piecewise-defined function.

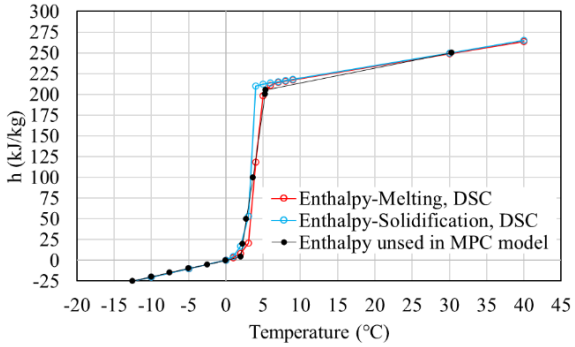

Figure 2:. PCM specific enthalpy profile changed with its temperature

Table 1: Thermal properties of PCM in TES unit

Thermal property	Latent heat (J/g)	Freezing temperature (°C)	Melting temperature (°C)	Thermal conductivity (W/m K)	Specific heat (kJ/kg K)	Density (g/cm3)
Parameter	175.88(Melting) 180.12(Freezing)	3	5	0.15 (Liquid) 0.23 (Solid)	1.7	0.87

2.3 Control strategies

Electric Time-of-Use (TOU) rates are a critical consideration in implementing control strategies. The electric rate during the on-peak period from 2 to 4 pm is \$0.226/kWh, while the rate for the off-peak period is \$0.042/kWh. Two control strategies were evaluated in the field test: Rule-Based Control (RBC) and MPC. In this study, RBC serves as the baseline, with its control logic detailed in Table 2. The primary goal of RBC is to maintain the thermostat at 22°C and minimize compressor power usage during peak hours. Therefore, the HP cooling mode is activated only if the room temperature exceeds 22°C and the TES temperature is above 12°C, indicating insufficient cooling storage. Conversely, during off-peak periods, RBC prioritizes charging the TES, as long as it remains within specified temperature constraints. As employed in the TES-HP system field test, this RBC transmits control mode selections to the system actuators at 10-minute intervals.

Table 2: RBC control logic

Current room temperature	On-peak period (2-4 pm)	Off-peak period
If T_{Room} > 22 °C	if T_{a_avg} > 12 °C: **HP cooling** if T_{a_avg} < 12 °C: **TES discharge**	**HP cooling**
If T_{Room} < 22 °C	**Standby**	if T_{a_avg} < 0 °C: **Standby** if T_{a_avg} > 0 °C: **TES charge**

The objective function is defined in Equation (1a), where k represents the time step variable; N denotes the total number of time steps in the prediction horizon; u represents the control output; P is the total power consumption of the TES-HP system at each time step; Δt is the sample time; and c is the electricity price at each time step. Equation (1b) describes the time-discretized system model, in which $\boldsymbol{x}$ denotes the system states, including room space temperature T_{room}, wall temperature T_{wall}, antifreeze tank temperature, T_{a_avg}, and energy accumulated in TES unit Q_{pcm} ; u comprises of four-mode selection, including HP cooling mode, TES charging mode, TES discharging mode and Standby mode; $\boldsymbol{d}$ denotes the disturbance including outdoor ambient temperature T_{amb}, solar radiation heat q_{sol}, solid temperature T_{sol}, and the electric rate price c. $\boldsymbol{x}_{lb}$ and $\boldsymbol{x}_{ub}$ are the lower boundary and upper boundary of the state variables. Specifically, the room temperature is constrained to a range of 16~18 °C.

$$\min_{u_1,u_2,\ldots,u_{N-1}} \sum_{k=1}^{N-1} P_k \cdot \Delta t \cdot c_k \tag{1a}$$

Subject to

$$\boldsymbol{x}_{k+1} = \boldsymbol{f}(\boldsymbol{x}_k, u_k, \boldsymbol{d}_k) \tag{1b}$$

$$\boldsymbol{x}_{lb,k} \leq x_k \leq x_{ub,k} \tag{1c}$$

$$\boldsymbol{x} = \left[T_{room} \;\; T_{wall} \;\; T_{a\_avg} \;\; Q_{pcm}\right] \tag{1d}$$

$\boldsymbol{u}$**:** Control mode. Selected from (1) HP cooling mode, (2) TES charge mode, (3) TES discharge mode, (4) standby mode (1e)

$$\boldsymbol{d} = [T_{amb} \;\; q_{sol} \;\; T_{sol} \;\; c] \tag{1f}$$

The control-oriented model as described in Equation (1b) consists of building RC model as given in Equation (2)-(3), and the TES-HP system model as given in Equation (4)-(5). For the building RC model, room temperature and the wall temperature are selected as the primary RC-network nodes. The thermal resistance including R_{wall1}, R_{wall2}, R_{win}, and $R_{102-105}$ are obtained based on experimental data; q_{AC} is the cooling capacity provided to the room space; q_{Sol} and q_{IHL} are the solar radiation heat and the internal heat gain, respectively; ε is the coefficient for the each heat transfer and obtained from experimental data. As for the TES unit model, T_{pcm} is a function of Q_{pcm}, which can be obtained by the function proposed in Section 2.1. q_{TES} is the heat transfer rate from hydronic loop to the antifreeze-PCM tank, which is calculated based on the tank inlet and the outlet temperature and flow rate. The lumped UA for the TES unit is calculated based on the experimental data and is a function of the TES temperature.

$$C_{in}\frac{\mathrm{d}T_{Room}}{\mathrm{d}t} = \frac{T_{Wall}-T_{Room}}{R_{wall1}} + \frac{T_{Amb}-T_{Room}}{R_{win}} + \varepsilon_1 \cdot q_{AC} + \varepsilon_2 \cdot q_{IHL} + \varepsilon_3 \cdot q_{Sol} + \frac{T_{in,102}-T_{room}}{R_{102}} + \frac{T_{in,103}-T_{room}}{R_{103}} + \frac{T_{in,105}-T_{room}}{R_{105}} \quad (2)$$

$$C_{Wall}\cdot\frac{\mathrm{d}T_{Wall}}{\mathrm{d}t} = \frac{T_{Sol}-T_{Wall}}{R_{wall2}} + \frac{T_{Room}-T_{Wall}}{R_{Wall1}} \quad (3)$$

$$\frac{\mathrm{d}T_{a\_avg}}{\mathrm{d}t} = M_a C_{p,a}\left[q_{TES} - (UA)_{a2p}\left(T_{a,avg} - T_{pcm}\right)\right] \quad (4)$$

$$\frac{\mathrm{d}Q_{pcm}}{\mathrm{d}t} = (UA)_{a2p}(T_{a,avg} - T_{pcm}) \quad (5)$$

The overall configuration and data flow of MPC are illustrated in Figure 3. The receding control horizon is set to 24 hours with a sampling interval of 10 minutes. At each sampling instant, Kalman filter is employed to estimate the wall temperature and the accumulated heat stored in the TES unit, according to the measured room temperature and the averaged antifreeze temperature. Dynamic programming (DP) is then applied to calculate an N-step sequence of control modes. However, only the control mode in the first step is executed by actuators. A new sequence $\boldsymbol{u}$ is calculated at the subsequent sampling time, incorporating both measured and estimated system states. This iterative process is repeated at each sampling instant to ensure that the most recent system states and forecast data inform each decision. Furthermore, at each sampling time, to increasing the accuracy of the system model as detailed in Equation (1b) and Equation (2)-(5), an internal calculation loop for the time-discretized model is executed with sample time (dt) of 60 seconds.

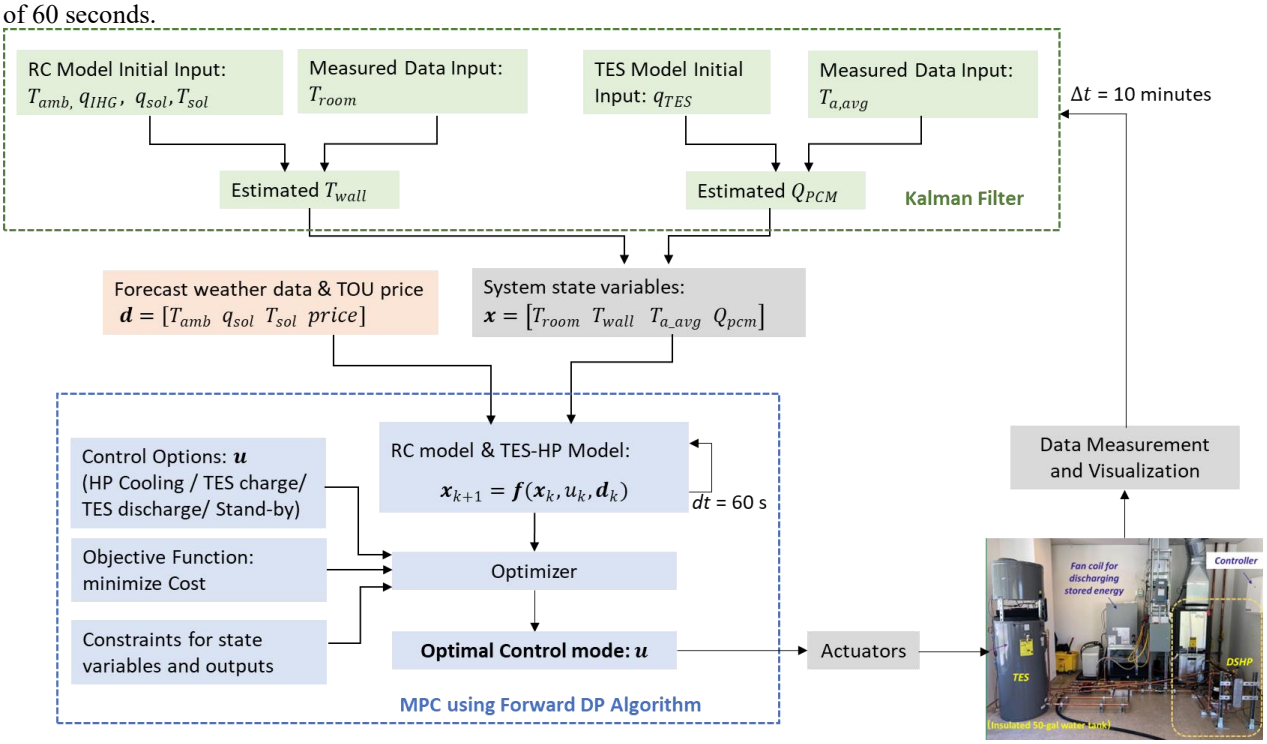

Figure 3: Overall MPC configuration and data flow

2.4 Evaluation index

To evaluate MPC and compare it with RBC, three perspectives are considered:

- **Using accumulated performance index**: Since MPC is designed to optimize system performance over a period rather than at specific instants, a comparative evaluation should focus on cumulative system performance. Therefore, accumulated Coefficient of Performance (COP) and Cooling Load per Cost (LpC) were calculated from field tests. The term 'accumulated' refers to the averaged performance from the beginning (t = 0) to the current time.

- **Eliminating HP system cooling mode and only comparing TES charge and discharge mode:** During the 2-day field test, there were periods when space cooling was provided by the HP mode, which can be considered as conventional HP operation without a TES unit. The COP or total electric cost in these cases may be influenced by ambient temperature and cooling load. Therefore, the comparison between MPC and RBC should primarily focus on the timing for charging and discharging the TES. The accumulated evaluation index thus excludes periods when the system ran in conventional HP cooling mode.

- **Considering performance index from both building and the HP system aspects.** The accumulated cooling load of the building space may not equal the cooling generated from the HVAC system, as a portion of cooling can be stored or released from the TES unit. Thus, the accumulated cooling capacity can be calculated from two perspectives: (1) from the building side, accumulated cooling is the sum of the discharging capacity from TES, i.e., $\sum_0^t Q_{discharge}(t)$; (2) from the HP system side, accumulated cooling is the sum of the charging capacity to TES, $\sum_0^t Q_{charge}(t)$.

Based on the aforementioned perspectives and considerations, the calculations for the index evaluation indices are presented in Equation (6)-(9), in which $\sum_0^t(.)$ represents the accumulated value from t = 0 to the current time t; 'building' indicates the building aspect, and 'HP' indicates the HP system aspect; only charge and discharge mode are accounted.

$$\mathrm{COP}_{building}(t) = \frac{\sum_0^t Q_{discharge}(t)}{\sum_0^t W_{charge}(t)} \quad (6)$$

$$\mathrm{COP}_{HP}(t) = \frac{\sum_0^t Q_{charge}(t)}{\sum_0^t W_{charge}(t)} \quad (7)$$

$$LpC_{building}(t) = \frac{\sum_0^t Q_{discharge}(t)}{\sum_0^t Cost_{charge}(t)} \quad (8)$$

$$LpC_{HP}(t) = \frac{\sum_0^t Q_{charge}(t)}{\sum_0^t Cost_{charge}(t)} \quad (9)$$

3. RESULT AND DISCUSSION

3.1 System operation

This section compares the system performance controlled by RBC and MPC strategies. The field test for both RBC and MPC started at 11:00 AM and continued for 48 hours in October 2023. Figure 4 shows the outdoor ambient temperature and the controlled building space temperature. It can be found that both control strategies can control the room temperature efficiently: RBC can maintain the room temperature consistently at 22 °C whereas MPC can keep the room temperature within a range of 16 ~ 18 °C.

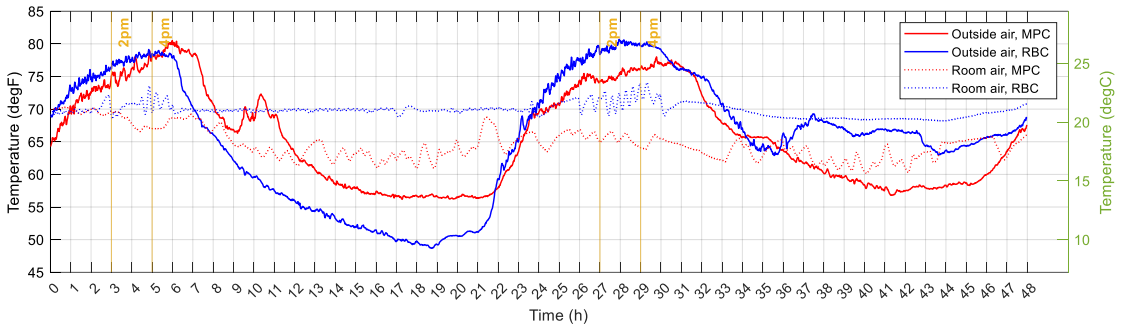

Figure 4: Building space temperature and the outdoor ambient temperature in the RBC and MPC field tests

The peak period, indicated by yellow lines in all figures, spans from 2 PM to 4 PM. Figure 5 depicts the TES charging rate, discharging rate, and the State of Charge (SOC) of the TES, while Figure 6 illustrates the instantaneous COP of the HP system during the TES charging process. It is observed that RBC charged the TES during the off-peak period (shown by the blue line) and discharged it during the peak period (shown by the green line), as detailed in Figure 6. On the second day, RBC began charging the TES unit from t = 29 hours, immediately following the off-peak hours. The corresponding SOC variation demonstrates a rapid decline during the peak hours and a gradual increase during the off-peak hours.

Unlike RBC, MPC discharged the TES unit less intensively throughout the entire period instead of only during on-peak times, and it selected optimal times for discharging and charging intelligently. For example, on the second day MPC chose to charge the TES at t = 34.5 hours, a time when the ambient temperature was lower, as indicated in Figure 4. This timing is advantageous as it likely results in a higher HP system COP. This benefit is evident in Figure 6, where the instantaneous COP for TES charging under RBC was 1.6 from 29 to 35 hours; however, for MPC, it exceeded 2.1 starting from t = 35 hours.

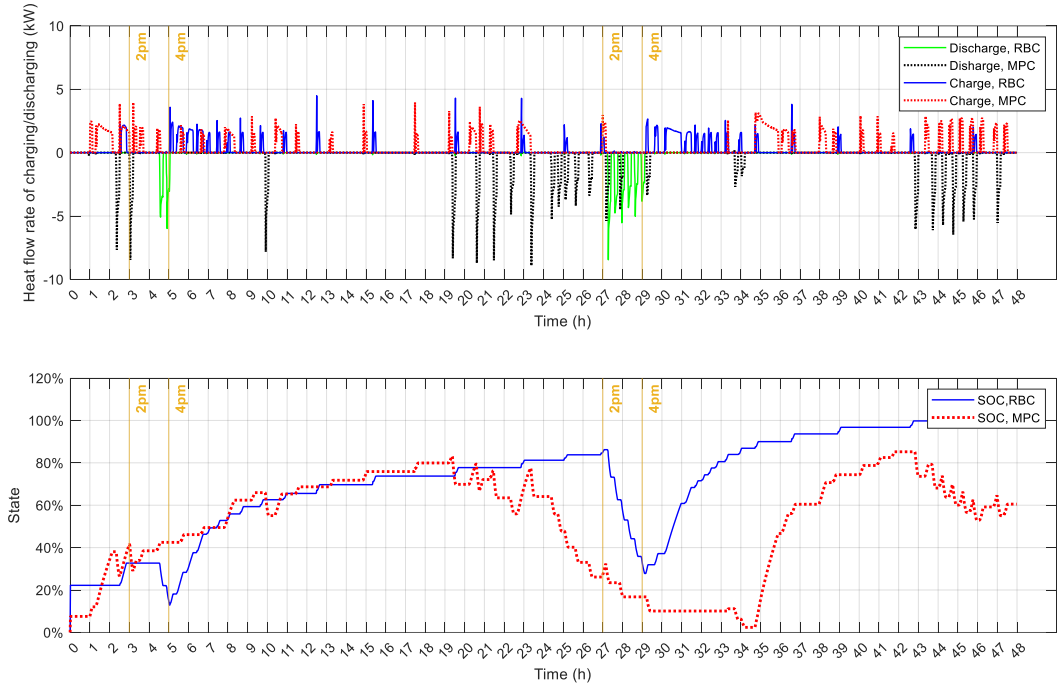

Figure 5: TES charging rate, TES discharging rate and SOC in the RBC and MPC field tests

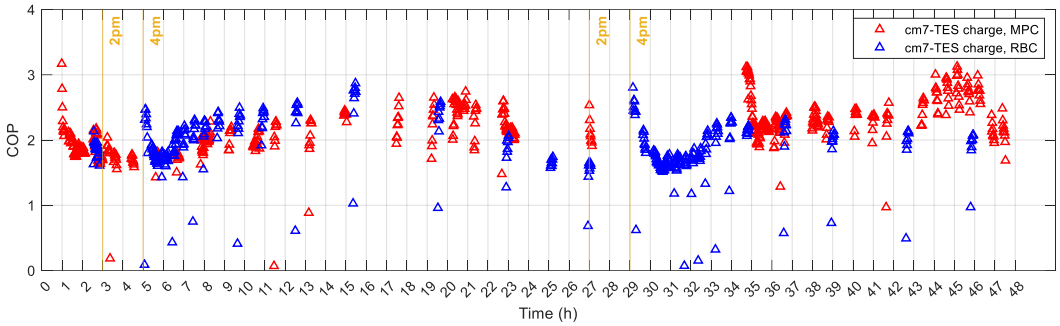

Figure 6: HP system COP during the TES charge mode for the RBC and MPC field tests

3.2 Performance evaluation

The average accumulated COP and LpC for both RBC and MPC are illustrated in Figure 7. The COP and LpC from HP system perspective are lower than those from the building perspective. This discrepancy arises because HP system generated more accumulated cooling capacity than the building cooling load, storing the extra cooling in the TES unit. Moreover, it can be noticed that during the peak hours, COP and LpC for RBC from the building aspect increased rapidly, because RBC applied the TES discharge mode to provide cooling to the building space. Furthermore, it is evident that after 35 hours, the averaged COP of MPC-based system was higher than that of RBC system. By the end of 48-hour period, the averaged COP of MPC system was 21.4 % higher than that of the RBC system. This improvement could be attributed to MPC's strategy of charging the TES according to the needs of the building and during periods of high instantaneous COP, such as when the outside ambient temperature was relatively low. Over time, it is also expected that the LpC of MPC can exceed that of RBC.

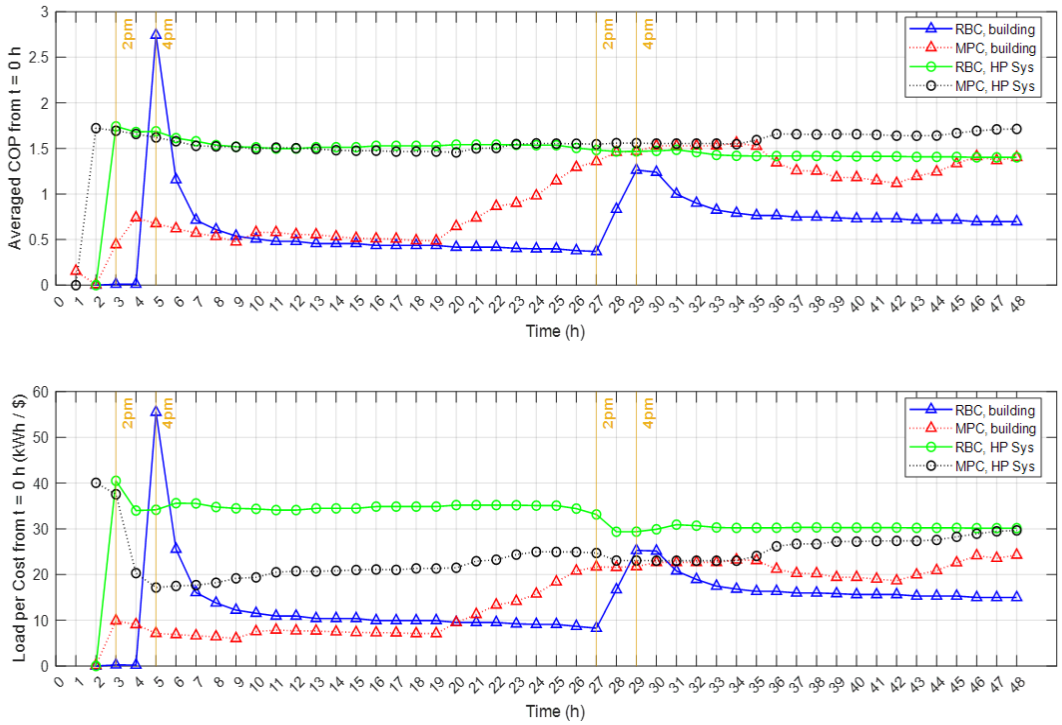

Figure 7: Accumulated averaged COP and LpC from building aspect and HP system aspect for both RBC and MPC field test.

4. CONCLUSIONS

This study evaluates the performance of MPC on a TES coupled with a HP system through field testing and comparison with the RBC strategy. The mode selection for the TES-HP system includes HP cooling, TES charging, TES discharging, and standby modes. The sequence of system modes during control periods is optimized by MPC using a DP algorithm. To implement MPC in the TES-HP setup, a control-oriented model comprising a building RC model and the TES unit model was developed, with the objective of minimizing electrical costs integrated into the MPC formulation. Results indicate that both MPC and RBC can effectively maintain the desired room temperature of the building space. Additionally, MPC intelligently selects when to charge and discharge the TES based on forecasted weather data and ToU rates. The accumulated COP at 48 hours shows a 21% increase with MPC compared to the baseline RBC. Over time, enhancements in both electrical cost and COP are anticipated to further improve.

REFERENCES

Cui, B. *et al.* (2022) 'Model predictive control for active insulation in building envelopes', *Energy and Buildings*, 267. doi: 10.1016/J.ENBUILD.2022.112108.

Dhumane, R. *et al.* (2019) 'Improving system performance of a personal conditioning system integrated with thermal storage', *Applied Thermal Engineering*, 147, pp. 40–51. doi: 10.1016/j.applthermaleng.2018.10.004.

Fu, Y. *et al.* (2023) 'How good are learning-based control v.s. model-based control for load shifting? Investigations on a single zone building energy system', *Energy*, 273(March). doi: 10.1016/j.energy.2023.127073.

Hirschey, J. *et al.* (2023) 'Demand reduction and energy saving potential of thermal energy storage integrated heat pumps', *International Journal of Refrigeration*, 148, pp. 179–192. doi: 10.1016/j.ijrefrig.2023.01.026.

Jin, X. *et al.* (2021) 'Optimal integration of building heating loads in integrated heating/electricity community energy systems: A Bi-Level MPC Approach', *IEEE Transactions on Sustainable Energy*, 12(3), pp. 1741–1754. doi: 10.1109/TSTE.2021.3064325.

Kim, D. *et al.* (2022) 'Site demonstration and performance evaluation of MPC for a large chiller plant with TES for renewable energy integration and grid decarbonization', *Applied Energy*, 321(November 2021), p. 119343. doi: 10.1016/j.apenergy.2022.119343.

Kuboth, S. *et al.* (2019) 'Economic model predictive control of combined thermal and electric residential building energy systems', *Applied Energy*, 240(January), pp. 372–385. doi: 10.1016/j.apenergy.2019.01.097.

Pangborn, H. C., Laird, C. E. and Alleyne, A. G. (2020) 'Hierarchical Hybrid MPC for Management of Distributed Phase Change Thermal Energy Storage', *Proceedings of the American Control Conference*, 2020-July, pp. 4147–4153. doi: 10.23919/ACC45564.2020.9147698.

Qiao, Y. *et al.* (2019) 'Experimental study of enhanced PCM exchangers applied in a thermal energy storage system for personal cooling', *International Journal of Refrigeration*, 102, pp. 22–34. doi: 10.1016/J.IJREFRIG.2019.03.006.

Qiao, Y. *et al.* (2020) 'Experimental study of a personal cooling system integrated with phase change material', *Applied Thermal Engineering*, 170, p. 115026. doi: 10.1016/j.applthermaleng.2020.115026.

Shi, L. *et al.* (2021) 'Potential of Utilizing Thermal Energy Storage Integrated Ground Source Heat Pump System to Reshape Electricity Demand in the United States', *ASME Journal of Engineering for Sustainable Buildings and Cities*, 2(3), pp. 1–13. doi: 10.1115/1.4051992.

Stritih, U. *et al.* (2018) 'Integration of passive PCM technologies for net-zero energy buildings', *Sustainable Cities and Society*, 41, pp. 286–295. doi: 10.1016/j.scs.2018.04.036.

Tarragona, J. *et al.* (2020) 'Economic evaluation of a hybrid heating system in different climate zones based on model predictive control', *Energy Conversion and Management*, 221(April), p. 113205. doi: 10.1016/j.enconman.2020.113205.

Tarragona, J. *et al.* (2021) 'Systematic review on model predictive control strategies applied to active thermal energy storage systems', *Renewable and Sustainable Energy Reviews*, 149, p. 111385. doi: 10.1016/j.rser.2021.111385.

Wang, J. *et al.* (2018) 'Application of model-based control strategy to hybrid free cooling system with latent heat thermal energy storage for TBSs', *Energy and Buildings*, 167, pp. 89–105. doi: 10.1016/j.enbuild.2018.02.036.